Nuclear Instruments and Methods in Physics Research A 858 (2017) 101–105

Contents lists available at ScienceDirect

Nuclear Instruments and Methods in Physics Research A

journal homepage: www.elsevier.com/locate/nima

Single- and multi-foils ^{27}Al(p,3pn)^{24}Na activation technique for monitoring the intensity of high-energy beams

A. Curioni[a,b], R. Froeschl[a], M. Glaser[a], E. Iliopoulou[a,c], F.P. La Torre[a], F. Pozzi[a,*], F. Ravotti[a], M. Silari[a]

[a] CERN, 1211 Geneva 23, Switzerland
[b] Politecnico di Milano, Department of Energy, 20156 Milan, Italy
[c] Medical Physics Laboratory, School of Medicine, Aristotle University of Thessaloniki, Greece

ARTICLE INFO

Keywords:
Hadron beam
Foil activation
IRRAD proton facility

ABSTRACT

This paper discusses an experimental study of the spallation reaction ^{27}Al(p,3pn)^{24}Na in Al foils exposed to 24 GeV c^{-1} protons, in the context of monitoring the intensity of multi-GeV proton beams through foil activation techniques. Since this reaction is sensitive to secondary neutrons and other energetic secondary hadrons, it is important to evaluate the impact of the foil thickness on the calculation of the beam intensity. This effect is determined experimentally using a stack of Al foils of varying thickness. The experimental results are then compared to Monte Carlo simulations.

1. Introduction

Different methods can be employed to measure the intensity of high-energy proton beams [1,2]. Among the devices used for this task are: Faraday cups [1,3] measuring the electrical charge of the beam, beam current transformers (BCTs) [4,5] measuring the magnetic field induced by the charged beam, as well as scintillators [6,7], ionisation chambers [8,9] and secondary electron emission chambers (SECs) [10,11] that measure the energy deposited by the beam in matter. Each technique has some limitations: Faraday cups are destructive and show peak power issues; BCT work only at high beam currents and are generally employed for pulsed beams; scintillators are not radiation hard and present saturation effects above a certain threshold; ionisation chambers generate very low outputs; SECs are usually employed for intensities of at least few hundred pA.

For the proton irradiation facility IRRAD[1] [12] located in the East Experimental Area of the CERN Proton Synchrotron (PS), the beam intensity to which samples are exposed is measured by a SEC. Since the samples can be smaller than the transverse area of the beam and to allow a sample-specific measurement, the conventional techniques listed above are not suited but a thin aluminium foil exactly covering the sample area is attached to each sample. Therefore, the total number of protons impinging on the samples is measured by the activation (determined by γ-spectrometry measurements) of the aluminium foil [13]. This technique is also used to calibrate active instrumentation [14].

This paper is based on a previous work on the foil activation technique [14] and discusses the use of this method to monitor the total number of protons at the IRRAD facility, the intensity of which is a factor of 1000 higher than that of ref [14]. The main focus of this paper is on the activation of aluminium foils and the experimental evaluation of the impact of the foil thickness on the calculation of the beam intensity, due to activation reactions induced by secondary neutrons and other energetic secondary hadrons. The experimental results are compared to FLUKA [15,16] Monte Carlo simulations that offer insight into reactions induced by secondary particles.

2. Material and methods

2.1. Calculation of the total number of protons

If $t = t_{IRR}+t_{WAIT}$, where t_{IRR} is the irradiation time and t_{WAIT} the waiting time, i.e. the time between the end of the irradiation and the γ-spectrometry measurement, the production rate at time t of ^{24}Na by the ^{27}Al(p,3pn) spallation reaction is:

$$A(t) = \frac{N_A}{M} \cdot \rho . \sigma . x . I . (1-e^{-\lambda t_{IRR}}) . e^{-\lambda t_{WAIT}} \quad (1)$$

where N_A is the Avogadro's number (mol^{-1}), M is the molar mass of aluminium (g·mol^{-1}), ρ is the aluminium density (g·cm^{-3}), σ is the production cross section (cm^2) of ^{24}Na, x is the foil thickness (cm), I is

* Corresponding author.
E-mail address: fabio.pozzi@cern.ch (F. Pozzi).
[1] www.cern.ch/ps-irrad

http://dx.doi.org/10.1016/j.nima.2017.03.058
Received 15 November 2016; Received in revised form 16 March 2017; Accepted 30 March 2017
Available online 31 March 2017

the average beam intensity in protons per second and λ is the ^{24}Na decay constant (s^{-1}). If σ is known for the specific beam energy, from Eq. (1) one can calculate I as:

$$I = \frac{A(t)}{\frac{N_A}{M}.\ \rho.\ \sigma.\ x.(1-e^{-\lambda t_{IRR}}).e^{-\lambda t_{WAIT}}} \quad (2)$$

Since no cross section data for protons are available in the literature at 24 GeV c^{-1} (the IRRAD proton beam energy), the value at 28 GeV measured by Cumming [17], i.e. (8.60 ± 0.34) mb, was used in Eq. (2). The activity, $A(t)$, is measured by γ-spectrometry, t_{IRR} and t_{WAIT} are recorded during the experiment. If the beam intensity is constant over the irradiation time one can calculate the total number of protons, P:

$$P = I.\ t_{IRR} \quad (3)$$

The production of ^{24}Na from ^{27}Al is sensitive to secondary neutrons, because of the competing ^{27}Al(n,α)^{24}Na reaction, and to the reactions induced by energetic secondary hadrons. The ^{27}Al(n,α)^{24}Na reaction has a threshold of 5.5 MeV and a cross section rising to 120 mb at 14 MeV [18]. Estimates of this effect in the literature vary between 0.25% per 100 mg cm^{-2} [19] to 1% per 100 mg cm^{-2} [20]. Since this contribution is in first order directly proportional to the total target thickness, it can be evaluated experimentally by activating foils of different thickness. To correct for this effect, one can fit the total number of protons calculated for each foil versus the mass thickness and extrapolate the total number of protons to zero thickness [14]. This is true if the foils are separately irradiated. If they are simultaneously irradiated, the activity in the downstream foils is influenced by secondary particles produced in the upstream ones. To account for this effect, for each foil one should sum the activity of all the upstream foils and, as thickness, consider the combined thickness of all foils. For instance, if three foils (denoted 1, 2 and 3) are irradiated in a stack, the relevant quantities for mass thickness x_m and activity are the following:

$$\begin{aligned} x'_{m1} &= x_{m1}\ ,\ \ A'_1 = A_1 \\ x'_{m2} &= x_{m1} + x_{m2}\ ,\ \ A'_2 = A_1 + A_2 \\ x'_{m3} &= x_{m1} + x_{m2} + x_{m3}\ ,\ \ A'_3 = A_1 + A_2 + A_3 \end{aligned} \quad (4)$$

From the new quantities x' and A' one can calculate the total number of protons for each foil combination by means of expressions (2) and (3). The contribution of secondary particles to the induced activity can then be evaluated through a linear regression of x' and P.

Another effect to be taken into account is the production of recoil nuclei. Some of the nuclei produced in the spallation process will have enough energy to leave the foil in the forward direction with respect to the primary beam. In this case they would not contribute to the foil activity. If a sandwich configuration with three foils (two 10 μm thick catchers and one thick central foil) is employed, in the central foil this effect is compensated by recoils received from the upstream one.

2.2. IRRAD proton facility

In high-energy physics facilities such as those at the CERN Large Hadron Collider (LHC) and its planned High-Luminosity upgrade (HL-LHC), devices are required to withstand a certain radiation level. As a result, detector materials and electronics components must be irradiated to test their radiation tolerance. To perform these irradiations, CERN built a new irradiation facility in the East Experimental Area at the PS. At this facility, named IRRAD, a Gaussian 24 GeV c^{-1} proton beam of variable size ranging from 5×5 mm^2 to 20×20 mm^2 (FWHM) is used for irradiation experiments. The IRRAD beam is delivered by the PS in "spills" with a maximum intensity of $5{\cdot}10^{11}$ protons per spill of about 400 ms duration. Several spills per PS super cycle (CPS) can be delivered to IRRAD resulting in a variable beam intensity depending on the number of users simultaneously served by the whole CERN accelerator complex. The detailed layout of IRRAD is shown in the Appendix A [12].

During irradiation it is necessary to monitor the intensity and the transverse profile of the proton beam in real-time. This is achieved by using a set of Beam Profile Monitors (BPMs) especially developed for this purpose [21], which only provide a relative measurement of the beam intensity. Moreover, the material directly installed in front of them in the beamline often influences their response. Finally, the samples are often irradiated in steps making the follow-up of the irradiation experiment complicated by using only the installed beam instrumentation. For the above reasons, and to provide an absolute determination of the proton beam intensity, the ^{27}Al(p,3pn)^{24}Na activation reaction is preferred. During each irradiation a single aluminium foil is placed in the beam together with the sample or device under test. The number of particles impinging on the foil is derived from the measurement of the ^{24}Na activity generated in the foil via γ-spectrometry. Due to the short half-life of ^{24}Na (~15 h), this procedure is limited to comparatively short irradiations of maximum 12 h. For long irradiation experiments (weeks or months), the ^{27}Al(p,3p3n)^{22}Na reaction is instead preferred due to the longer half-life of ^{22}Na (~2.6 years) and its lower sensitivity to secondary neutrons [13].

2.3. Experimental set-up

Four sandwiches of hyper-pure (99.999%) Al foils manufactured by Goodfellow, UK (www.goodfellow.com), with dimensions 50×50 mm^2 were installed in the irradiation area. Each sandwich was composed of two catchers (2.71 mg cm^{-2}) upstream and downstream of the central foil; the four central foils had the following mass thicknesses: 66.7, 139.0, 277.0 and 569.1 mg cm^{-2}. A single Al foil (27.1 mg cm^{-2} thick, 50×50 mm^2 and 99.5% purity) was also added to the set-up to compare the multi-foils technique with the single-foil technique. All sets of foils were inserted and centred with respect to the proton beam by using a dedicated support (slide-holder) installed on one of the irradiation tables in the Zone 1 of the IRRAD facility as shown in Fig. 1 (see also Appendix A) [22]. The foils were placed in order of increasing thickness. By using the BPM located upstream of IRRAD, the beam size at the measurement position was measured to be ~11×11 mm^2 (FWHM), smaller than the foil dimensions so that all beam particles hit the foils (Fig. 2). The irradiation was performed by setting a constant rate of one spill per PS super cycle and lasted about 22 min to reach the desired proton fluence. Since the intensity variation per spill recorded by the SEC is small (maximum of about 10%) the proton fluence was considered constant. In addition, a variation in the proton fluence has a negligible impact on the results, since the half-life of ^{24}Na is much longer than the irradiation time.

3. Results and discussion

3.1. Experimental results

The second column of Table 1 lists the activity of each Al foil measured by γ-spectrometry at the end of the irradiation. The standard deviations in Table 1 only take into account the uncertainty on the foil activity provided by the γ-spectrometry, which was in the order of 4% for the sandwich configuration and 7% for the 27.1 mg cm^{-2} foil. It does not include the 4% uncertainty on the proton cross section, which is common to all foils and was added to the final results. The third and fourth columns of Table 1 show the mass thickness and activity calculated from Eq. (4), to be used in Eqs. (2) and (3) to obtain the total number of protons (fifth column).

The total number of protons derived from the five foils were then

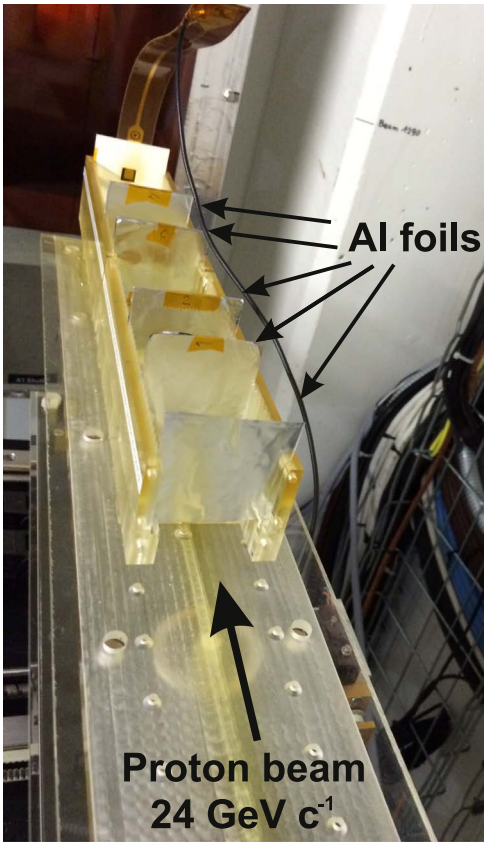

Fig. 1. Experimental set-up.

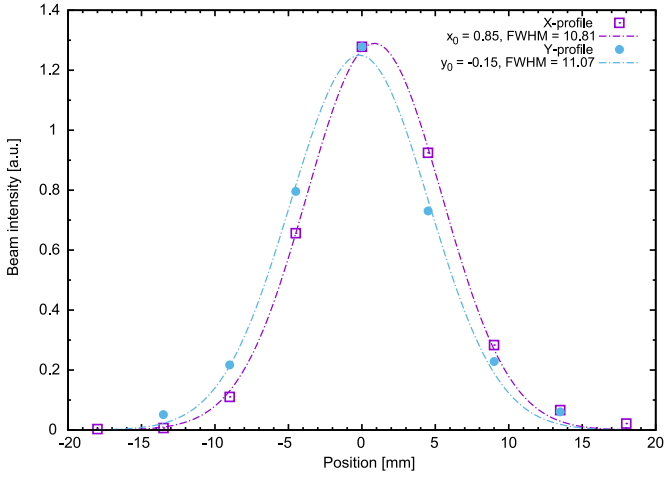

Fig. 2. Example of a beam profile measurement in transverse plane, X (purple squares) and Y (light blue dots) coordinates, together with the respective Gaussian fits. (For interpretation of the references to color in this figure legend, the reader is referred to the web version of this article.)

Table 1
24Na activity of each foil (2nd column) together with the quantities given by Eq. (4), which account for the simultaneous irradiation of the foils (3rd and 4th columns). The 5th column is the total number of protons derived from each foil combination.

x_m (mg cm^{-2})	*A (Bq)*	x'_m (mg cm^{-2})	*A′(Bq)*	*P (Protons)*
27.1	697.0 ± 46.7	27.1	697.0 ± 46.7	(1.051 ± 0.070)·10^{13}
66.7	1740.0 ± 80.0	93.8	2437.0 ± 92.7	(1.062 ± 0.040)·10^{13}
139.0	3660.0 ± 159.2	232.8	6097.0 ± 184.2	(1.070 ± 0.032)·10^{13}
277.0	7790.0 ± 346.7	509.8	13,887.0 ± 392.6	(1.113 ± 0.031)·10^{13}
569.1	178,00.0 ± 783.2	1078.9	31,687.0 ± 876.1	(1.200 ± 0.033)·10^{13}

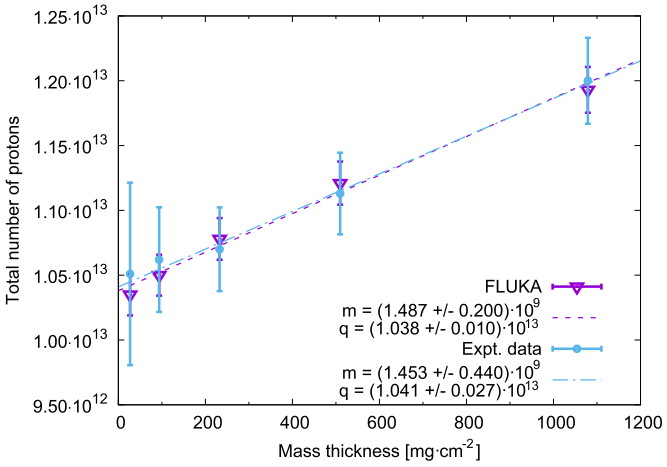

Fig. 3. Total number of protons calculated for the foil combinations (Eq. (4), see Table 1) together with the linear fit (see text) for both the experiment (light blue dots) and simulation (purple triangles). The y-error bars take into account only the standard deviation on the foil activity. (For interpretation of the references to color in this figure legend, the reader is referred to the web version of this article.)

Table 2
Total number of protons calculated with the single- and multi-foils techniques. The standard deviations also take into account the uncertainty on the cross section.

Method	***Φ (Protons)***
Single-foil	(1.051 ± 0.082)·10^{13}
Multi-foils	(1.041 ± 0.050)·10^{13}

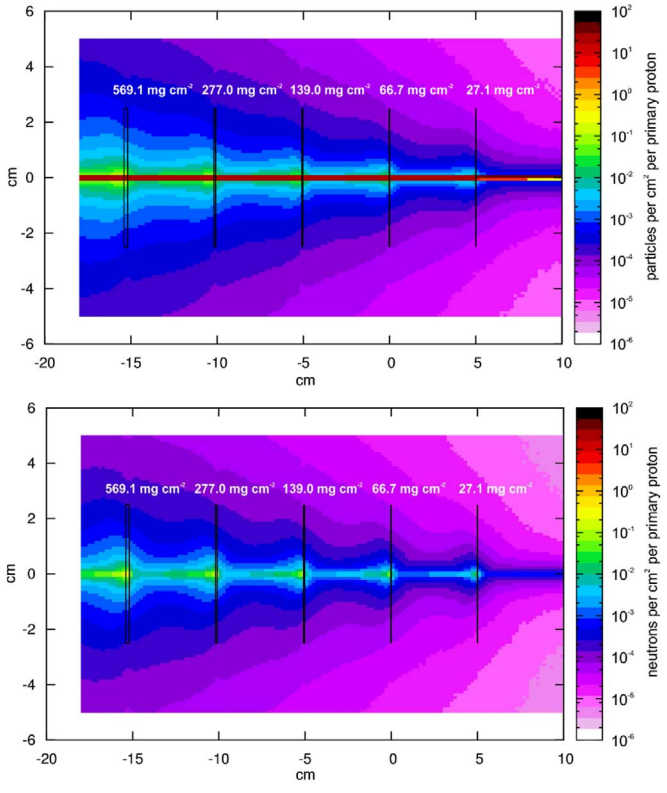

Fig. 4. FLUKA simulations. Top: Top-view of the fluence of protons, positive pions and neutrons (per cm^{-2} per primary proton) produced by the beam in the experimental set up. Bottom: top-view of the neutron fluence (per cm^{-2} per primary proton) produced by the beam. The beam travels from right to left.

Table 3
^{24}Na production yield for each foil (2nd column). The 3rd and 4th columns list mass thickness and ^{24}Na production yield for each foil combination Eq. (4). The 5th column is the total number of protons after the normalization (see text). The uncertainties on the activity and on P are not listed since always below 0.5%.

x_m (mg cm^{-2})	Y (Yield per primary proton)	x'_m (mg cm^{-2})	Y' (Yield per primary proton)	P_{NORM} (Protons)
27.1	$2.42\cdot10^{-6}$	27.1	$2.25\cdot10^{-6}$	$(1.035 \pm 0.016)\ 10^{13}$
67.8	$6.08\cdot10^{-6}$	93.8	$8.50\cdot10^{-6}$	$(1.050 \pm 0.016)\ 10^{13}$
135.5	$1.32\cdot10^{-5}$	232.8	$2.17\cdot10^{-5}$	$(1.078 \pm 0.016)\ 10^{13}$
271.0	$2.76\cdot10^{-5}$	509.8	$4.93\cdot10^{-5}$	$(1.121 \pm 0.017)\ 10^{13}$
542.0	$6.17\cdot10^{-5}$	1078.9	$1.11\cdot10^{-4}$	$(1.193 \pm 0.018)\ 10^{13}$

fitted with a linear function to extrapolate the value to zero thickness, which represents the total number of protons from the multi-foils technique. Fig. 3 shows the experimental data and the results of the Monte Carlo simulations discussed in the next section, together with the linear fit. Table 2 lists the total number of protons obtained with the single- and multi-foils techniques.

The two techniques provide consistent values for the total number of protons within the respective uncertainties. The contribution of secondary particles to the induced activity was calculated as explained in section 4.1.1 of ref. [14] (the ratio m/q of the fitting parameters in Fig. 3), obtaining a value of 1.4% per 100 mg cm^{-2}, fully consistent with the values present in the literature. Therefore, only 0.4% of the activity of the 27.1 mg cm^{-2} foil is induced by secondary particles. The effect is negligible for the single-foil technique (where it is not taken into account) if compared with the uncertainty on the activity. It should also be noted that secondary particles contribute to less than 2% of the total activity for foils up to a mass thickness of about 140 mg cm^{-2}, whereas for thicker foils this contribution is comparable or even higher than the uncertainty on the activity; in this case the multi-foils technique must be employed to correct for it.

3.2. Comparison with Monte Carlo simulations

FLUKA [15,16] Monte Carlo simulations were employed to assess the contribution of neutrons and energetic secondary hadrons to the induced activity and compare it with the experimental results. The experimental set-up was reproduced by simulating five Al foils (27.1, 66.7, 139.0, 277.0 and 569.1 g cm^{-2}) irradiated by a 24 GeV c^{-1} proton beam (Fig. 4). The production yield of ^{24}Na was estimated in semi-analogue mode, i.e. each single radioactive nucleus was treated in a Monte Carlo way like all other unstable particles (for more details see ref. [16]). Table 3 lists the production yield of ^{24}Na, Y, together with mass thickness, production yield (Y') and total number of protons for each combination of foils calculated as in Section 3.1. By means of a linear regression as done for the experimental results, the contribution of secondary particles to the induced activity was calculated. This is 1.4% per 100 mg cm^{-2}, in excellent agreement with the experimental value (Fig. 3). The values in column 4 of Table 3 are normalized per primary FLUKA proton and cannot be directly compared to the experimental measurements. In order to normalize the FLUKA results, the following quantities were calculated:

a) ratio between experimental activity and simulated production yield for each combination of foils;
b) standard deviation for each ratio of point (a);
c) weighted average of the ratios calculated in point (a), resulting in $(2.838 \pm 0.042)\cdot10^{8}$ primary protons;
d) normalization of the total number of protons from FLUKA by means of the factor calculated in (c) (the results are summarized in column 5 of Table 3).

4. Conclusions

The single- and multi-foils aluminium activation techniques were investigated and compared at the CERN IRRAD facility to measure the total number of protons impinging on the foils. The two techniques showed consistent results within the respective uncertainties; the single-foil (27.1 mg cm^{-2}) technique is confirmed to be the first choice for measuring the total number of protons when the beam intensity is sufficiently high, e.g. 10^{10} protons per second, to induce a measurable activity of ^{24}Na. In addition, single foils up to 140 mg cm^{-2} can be employed since the contribution of energetic secondary hadrons is less than 2% of the total ^{24}Na activity. If much lower beam intensities have

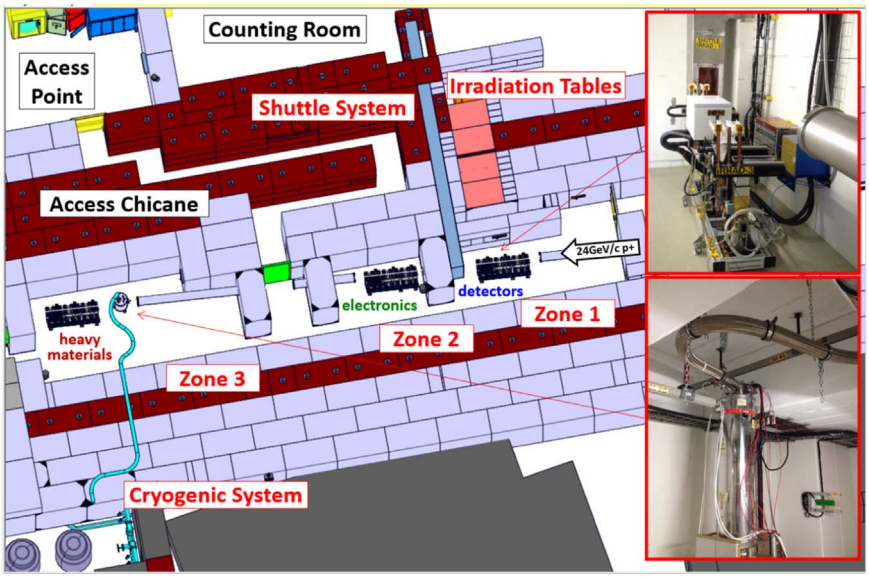

Fig. 5. Layout of the IRRAD proton irradiation facility.

to be measured, thicker foils should be employed, with which the contribution of secondary reactions becomes comparable to the activity uncertainty. Therefore, the multi-foils technique must be employed and the extrapolation to zero thickness will provide a good estimate of the total number of protons. The capability of the FLUKA code to reproduce secondary reactions was also investigated confirming its reliability as a tool for studying and planning activation experiments.

Appendix: A

The detailed layout of the IRRAD proton irradiation facility is shown in Fig. 5. From right to left, three groups of remote-controlled tables allow positioning the samples in the beam line or close to it. Low-Z samples as thin silicon devices are irradiated on the upstream tables (Zone 1), while the highest-Z samples, such as dense calorimetry material, downstream (Zone 3). The intermediate group of tables (Zone 2) is typically used for the irradiation of electronics equipment. Small objects can be moved from outside IRRAD to the irradiation position via a shuttle system [12]. Every IRRAD zone is equipped with a patch-panel to provide the IRRAD users with the possibility to perform on-line measurements during irradiation. Finally, in the downstream Zone 3, one table is equipped with a cryostat filled with liquid helium allowing special irradiation runs with samples exposed at cryogenic temperatures down to 1.8 K.

References

[1] D. Yount, Nucl. Instrum. Methods 52 (1) (1967) 1–14.
[2] P. Forck, Beam Current Measurements, Lecture Given at the Joint Universities Accelerator School (JUAS), Archamps, France. Available at: ⟨http://www-bd.gsi.de/conf/juas/current_trans.pdf⟩, 2013.
[3] J. Harasimowicz, C.P. Welsch, Proceedings 2010 Beam Instrum. Workshop (BIW), Santa Fe, New Mexico, USA, 2010.
[4] H. Feist, M. Koep, H. Reich, Nucl. Instrum. Methods 97 (2) (1971) 319–321.
[5] J. Belleman, D. Belohrad, L. Jensen, M. Krupa, A. Topaloudis, Proceedings 2nd International Beam Instrum. Conference (IBIC), Oxford, 2013.
[6] L.L. Kanstein, R.E. Morgado, D.U. Norgren, R.W. Sorensen, Nucl. Instrum. Methods 118 (1974) 483–485.
[7] J.H. So, H.J. Kim, H. Kang, H. Park, S. Ryu, S.W. Jung, J. Korean Phys. Soc. 50 (95) (2007) 1506–1509.
[8] A.J. Metheringham, T.R. Willitts, Nucl. Instrum. Methods 15 (4) (1962) 297–299.
[9] H.S. Kim, S.H. Park, Y.K. Kim, J.H. Ha, S.M. Kang, C.E. Chung, J. Korean Phys. Soc. 48 (2) (2006) 213–217.
[10] B. Planskoy, Nucl. Instrum. Methods 24 (1963) 172–180.
[11] K. Bernier, G. de Rijk, G. Ferioli, E. Hatziangeli, A. Marchionni, V. Palladino, G.R. Stevenson, T. Tabarelli de Fatis, E. Tsesmelis, CERN Yellow Report. (1997) (97-07).
[12] F. Ravotti, et al.,Proceedings Twelfth International Top. Meet. Nucl. Appl. Accel. (AccApp'15). In press, 2015, also AIDA-2020-CONF-2016-006 (available on CERN CDS: ⟨http://cds.cern.ch/record/2237333?=ln=en⟩).
[13] F. Ravotti, M. Glaser, M. Moll, IEEE Trans. Nucl. Sci. 53 (2006) 2016–2022.
[14] A. Ferrari, F.P. La Torre, G.P. Manessi, F. Pozzi, M. Silari, Nucl. Instrum. Methods A 763 (2014) 177–183.
[15] T.T. Böhlen, F. Cerutti, M.P.W. Chin, A. Fassò, A. Ferrari, P.G. Ortega, A. Mairani, P.R. Sala, G. Smirnov, V. Vlachoudis, Nucl. Data Sheets 120 (2014) 211–214.
[16] A. Ferrari, P.R. Sala, A. Fassò, J. Ranft, CERN-2005-10, INFN/TC_05/11, SLAC-R-773, 2005.
[17] J.B. Cumming, Annu. Rev. Nucl. Sci. 13 (1963) 261–286.
[18] J.P. Butler, D.C. Santry, Can. J. Phys. 41 (2) (1963) 372–383.
[19] J.B. Cumming, J. Hudis, A.M. Poskanzer, S. Kaufman, Phys. Rev. 128 (5) (1962) 2392–2397.
[20] J.R. Grover, Phys. Rev. 126 (4) (1962) 1540–1554.
[21] M. Glaser et al., Proc. Twelfth Int. Topical Meeting on Nuclear Applications Acceleration (AccApp'15) . In press, 2015, also AIDA-2020-CONF-2016-004 (available on CERN CDS: http://cds.cern.ch/record/2235836?ln=en).
[22] M. Glaser, M. Moll, F. Ravotti, 2013, ⟨https://cds.cern.ch/record/1594787/files/AIDA-MS31.pdf⟩).